Supplementary information

To confirm the synthesis was successful, ^{1}H and ^{13}C NMR spectroscopy was used to characterise the salts. The NMR spectra for $Zn(MA)_2$ is in agreement with the expected spectra with three proton environments and four carbon environments detected, albeit with some impurities denoted with * in the spectra. The Elemental Analysis (EA) (*found below the NMR*) for $Zn(MA)_2$ revealed the C and H % were within 1.5% for C and 0.3 % for H of the calculated ratios. Meanwhile, Electrospray Ionisation Mass Spectrometry (ESI-MS) for $Zn(MA)_2$ detects the full protonated salt and a mass which is in-line with Zn(MA) (Fig. S2).

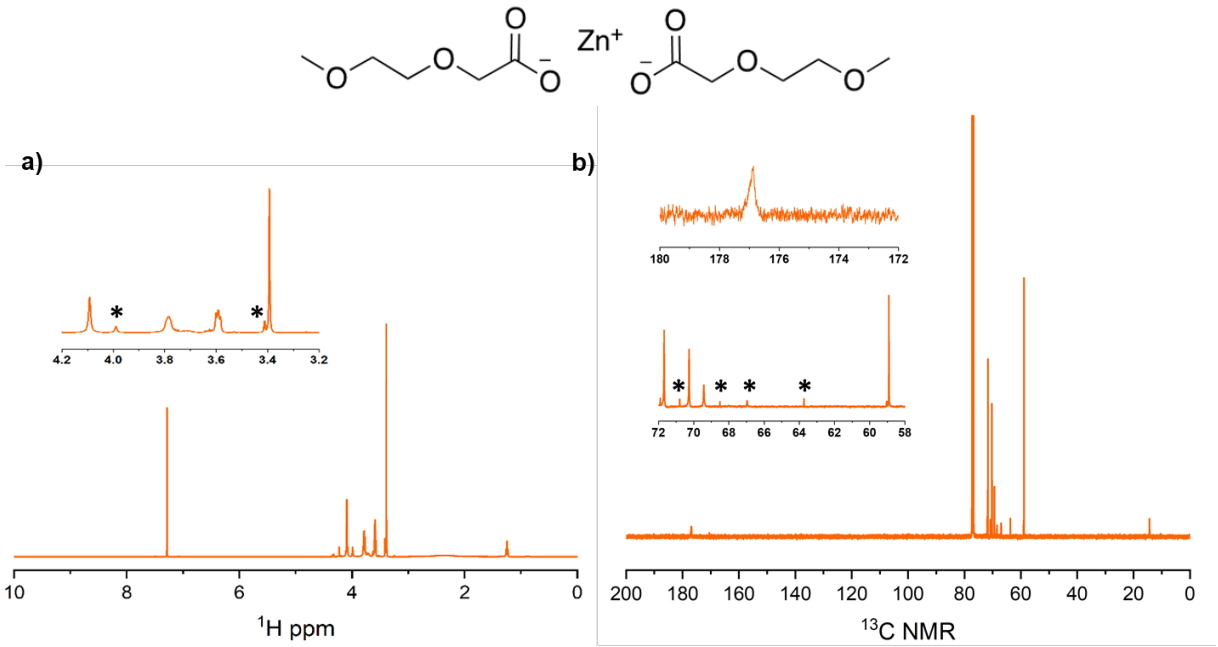

*Fig. S1 - a) ^{1}H NMR of $Zn(MA)_2$ * denotes impurities, most likely HMA precursor b) ^{13}C NMR of $Zn(MA)_2$ * denotes impurities, most likely HMA precursor.*

^{1}H-NMR (300 MHz, $CDCl_3$, TMS): ^{d}H: 3.4 (s, 6 H, CH_3), 3.55-3.81 (m, 8 H, CH_2), 4.11 (s, 4 H, C**H**$_2$COO$^-$)

^{13}C-NMR (300 MHz, $CDCl_3$, TMS): dC: 58.91 (2 C, CH_3), 69.42 (2 C, **C**H_2COO$^-$), 68.61 (2 C, **C**H_2OCH_3), 68.61 (2 C, CH_2O**C**H_2COO$^-$), 176.81 (2 C, **C**OO$^-$)

Elemental analysis: calculated: 36.22% C, 5.78% H; found: 34.88% C, 5.47% H

ESI-MS (DCM-MeOH, NH_4Ac): m/z (+p): 196.98 (20%, Zn(MA)H+), 331.04 (75%, Zn(MA)H+)

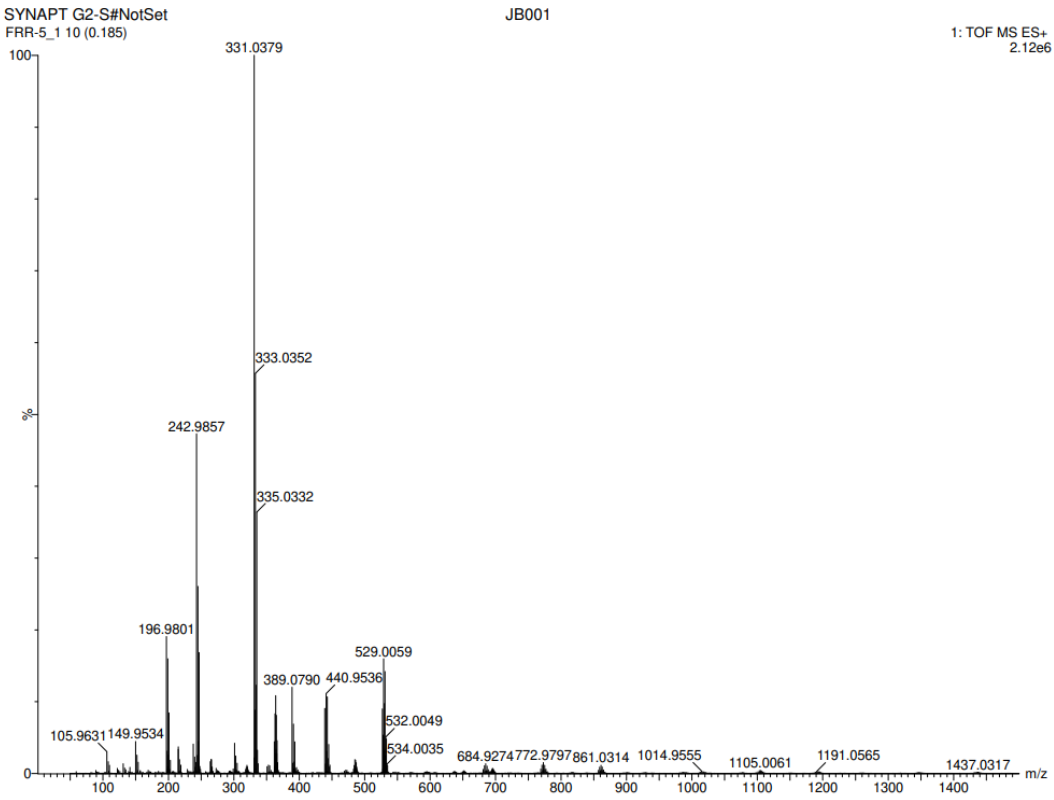

Fig. S2 - MS for $Zn(MA)_2$.

The NMR spectra for $Zn(MEA)_2$ is in agreement with the expected spectra with three proton environments and five carbon environments detected. There are some slight impurities, denoted with * in the spectra. The EA for $Zn(MEA)_2$ revealed the C and H % were within 1 % for C and 0.2 % for H of the calculated ratios. Meanwhile, ESI-MS for $Zn(MEA)_2$ detects the full protonated salt and a mass which is in-line with Zn(MEA) (Fig. S4).

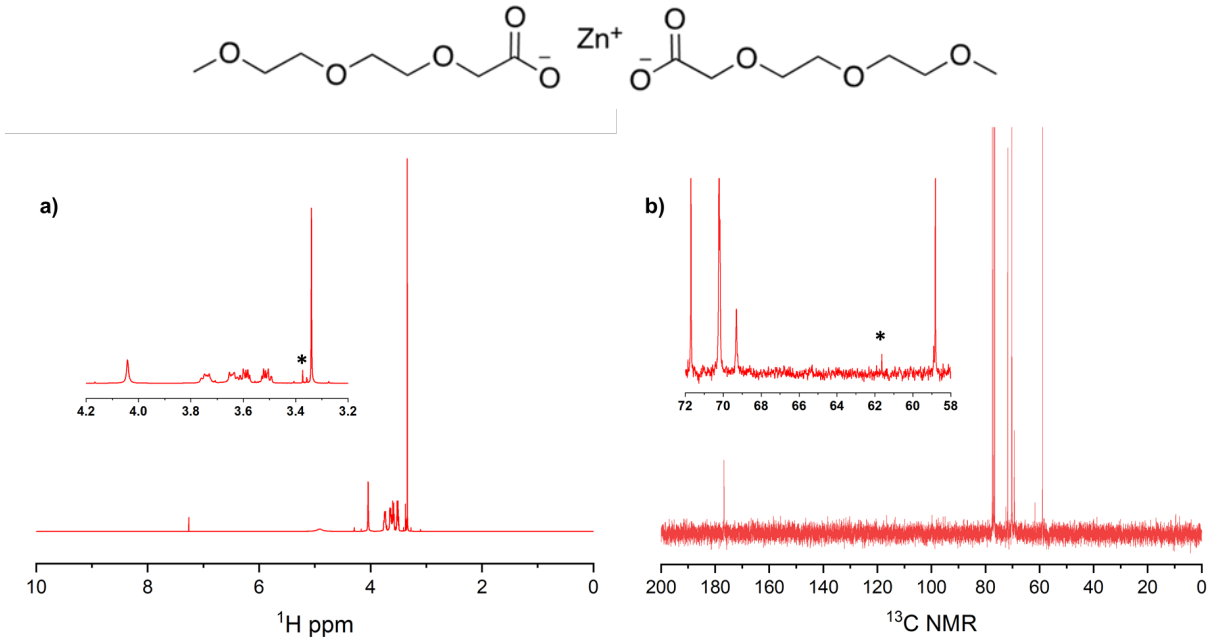

*Fig. S3 - a) ^{1}H NMR of $Zn(MEA)_2$ * denotes impurities, most likely HMEA precursor b) ^{13}C NMR of $Zn(MEA)_2$ * denotes impurities, most likely HMA precursor.*

^{1}H-NMR (300 MHz, $CDCl_3$, TMS): ^{d}H: 3.33 (s, 6 H, CH_3), 3.47-3.77 (m, 16 H, CH_2), 4.04 (s, 4 H, C**H**$_2$COOH)

^{13}C-NMR (300 MHz, $CDCl_3$, TMS): ^{d}C: 58.86 (2 C, CH_3), 68.61 (2 C, **C**H_2COO^-) 70.21 (6 C, CH_2), 71.72 (2 C, **C**H_2OCH_3),176.10 (2 C, **C**OO^-)

Elemental analysis: calculated: 40.06 % C, 6.24% H; found: 39.125% C, 6.546% H

ESI-MS (DCM-MeOH, NH_4Ac): m/z (+p): 241.01 (100%, Zn(MEA)H+), 419.09 (100%, $Zn(MEA)_2$H+)

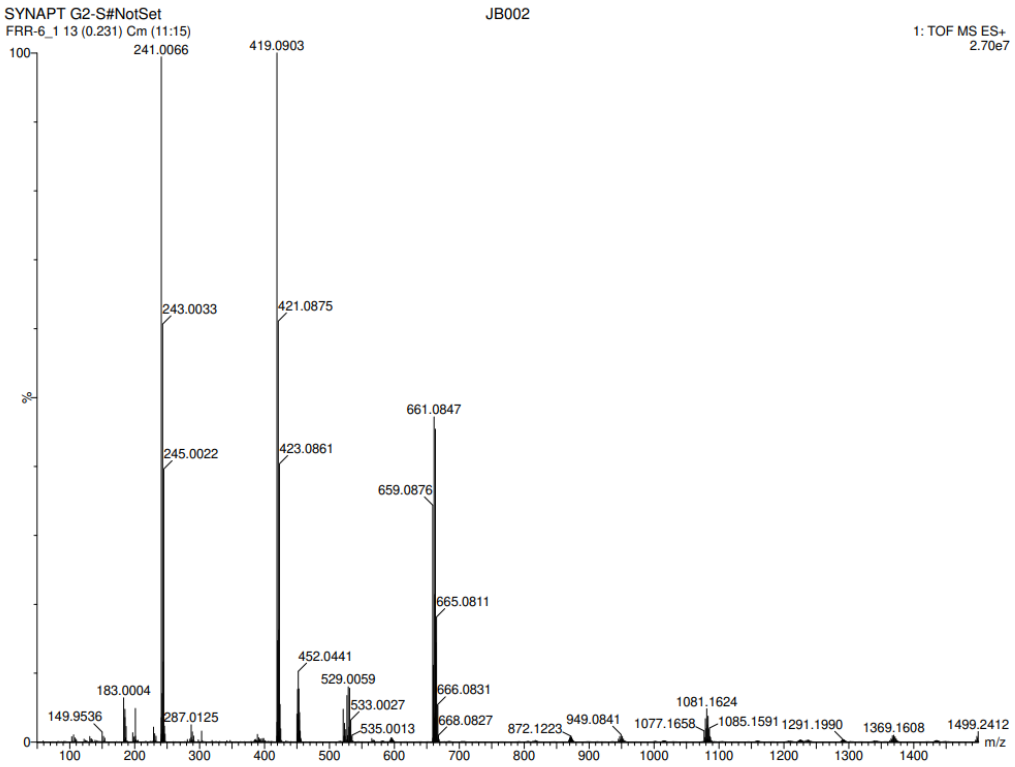

Fig. S4 - MS for $Zn(MEA)_2$.

The NMR spectra for $Zn(MEEA)_2$ is in agreement with the expected spectra with three proton environments and six carbon environments detected. The EA (*found* for $Zn(MEA)_2$ revealed the C and H % were within 1 % for C and 0.8 % for H of the calculated ratios. Meanwhile, ESI-MS for $Zn(MEEA)_2$ detects the full protonated salt and a mass which is in-line with Zn(MEEA) (Fig. S6)

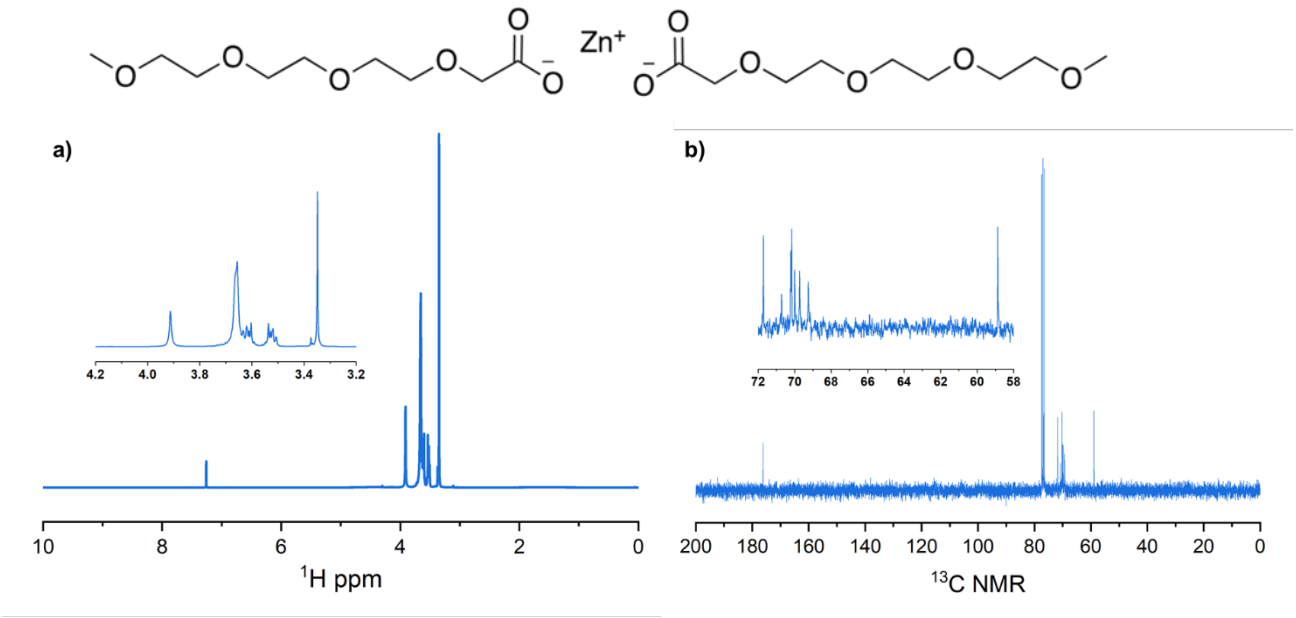

Fig. S5 - a) ^1H NMR of $Zn(MEEA)_2$ b) ^{13}C NMR of $Zn(MEEA)_2$.

^{1}H-NMR (300 MHz, $CDCl_3$, TMS): dH: 3.30 (s, 6 H, CH_3), 3.48-3.68 (m, 24 H, CH_2), 3.91 (s, 4 H, C**H**$_2$COO$^-$)

^{13}C-NMR (300 MHz, $CDCl_3$, TMS): dC: 58.86 (CH_3), 68.61 (**C**H_2COO$^-$), 69.95 –70.50 (8 C, CH_2), 71.14 (**C**H_2OCH_2COO$^-$), 71.77 (CH_3O**C**H_2), 176.10 (**C**OO$^-$)

Elemental analysis: calculated: 42.57% C, 6.75% H; found: 43.52% C, 7.56% H

ESI-MS (DCM-MeOH, NH_4Ac): m/z (+p): 285.03 (100%, Zn(MEEA)H+), 477.13 (100%, $Zn(MEEA)_2$-CH_2O) 507.14 (75%, $Zn(MEEA)_2$H+)

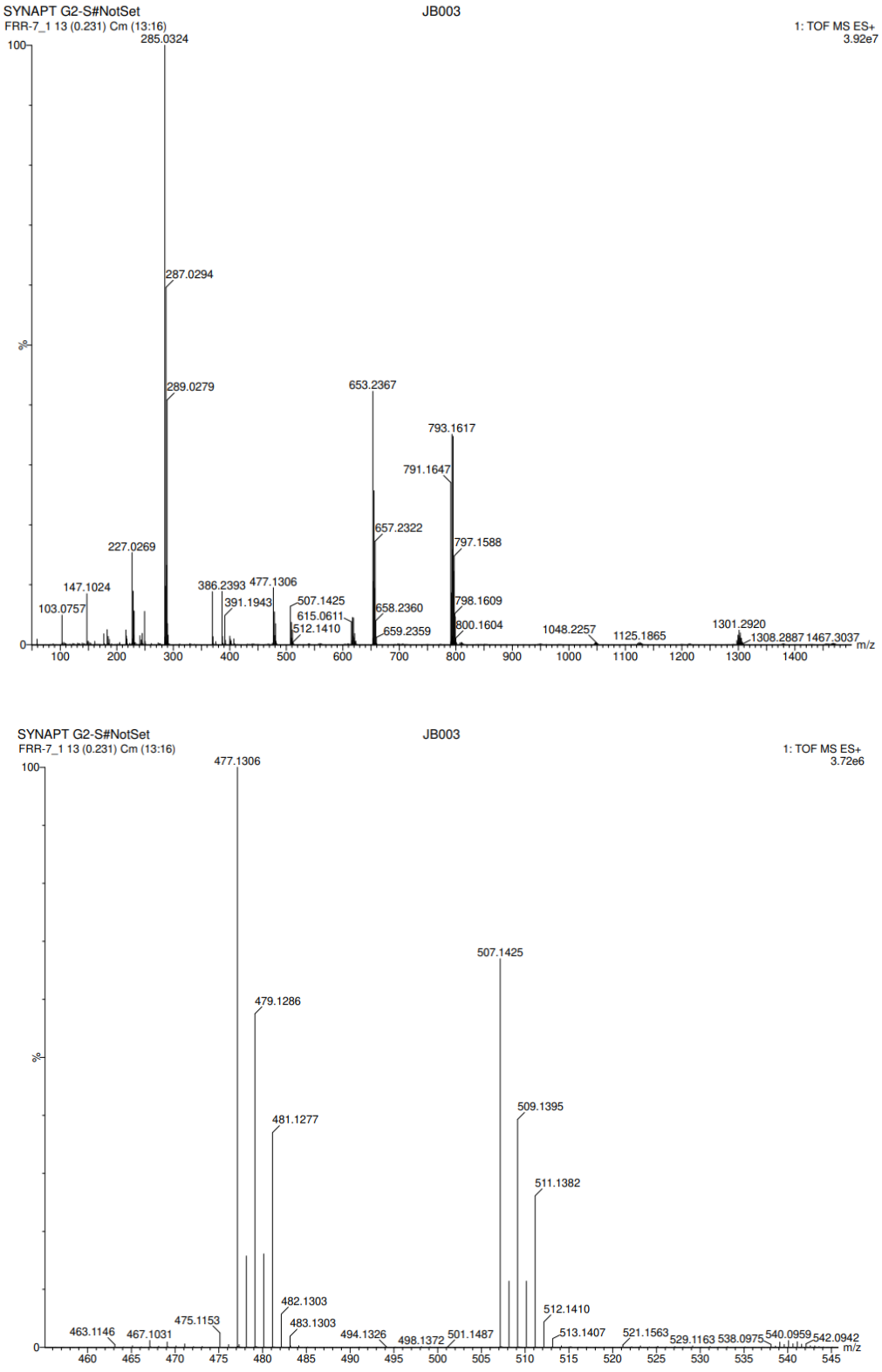

Fig. S6 - MS for $Zn(MEEA)_2$.

Based on the NMR, EA and MS data we are confident that the salts were all successfully synthesised. To further characterise the salts, differential scanning calorimetry (DSC) was used and revealed that melting and glass transition temperatures decrease with longer chains. $Zn(MA)_2$ has a glass transition temperature of 145 ºC, whereas $Zn(MEA)_2$ is technically an ionic liquid with a glass transition temperature of 97 ºC. $Zn(MEEA)_2$ has no discernible glass transition temperature, indicating that $Zn(MEEA)_2$ is a room temperature ionic liquid. Thermogravimetric analysis (TGA) demonstrated high thermal stability, with decomposition temperatures around 300ºC for all three salts.

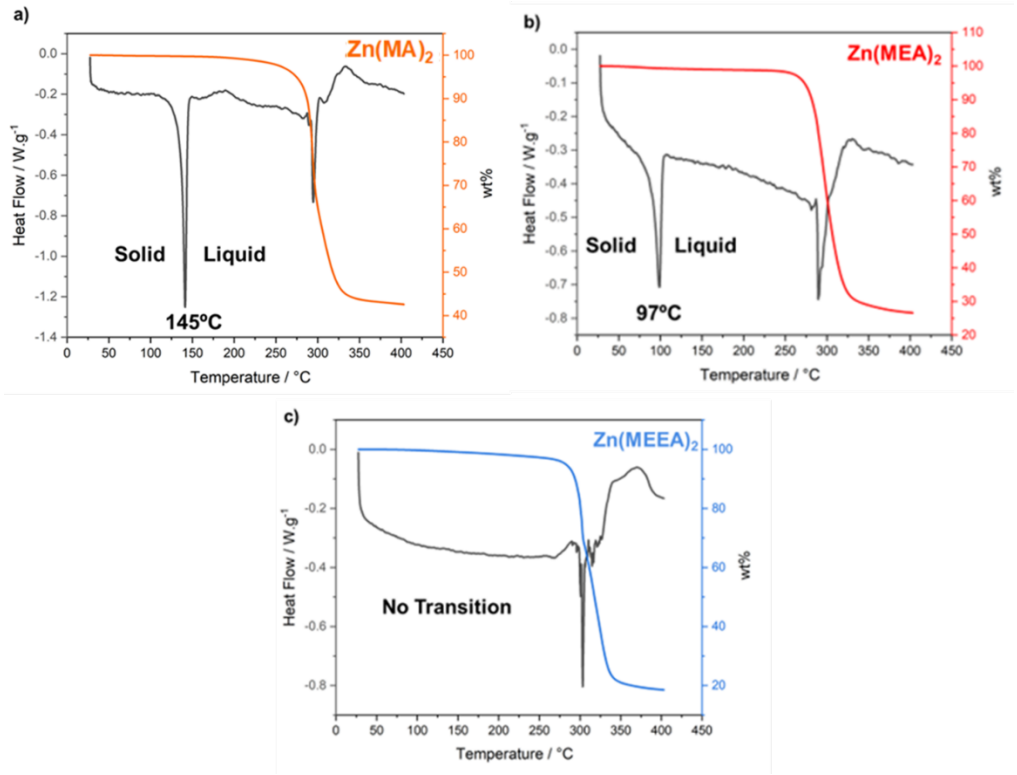

Fig. S7 – a) Differential scanning calorimetry (DSC) in grey and thermogravimetric analysis (TGA) in orange for $Zn(MA)_2$, b) DSC (grey) and TGA (red) for $Zn(MA)_2$ and c) DSC (grey) and TGA (red) for $Zn(MEEA)_2$.

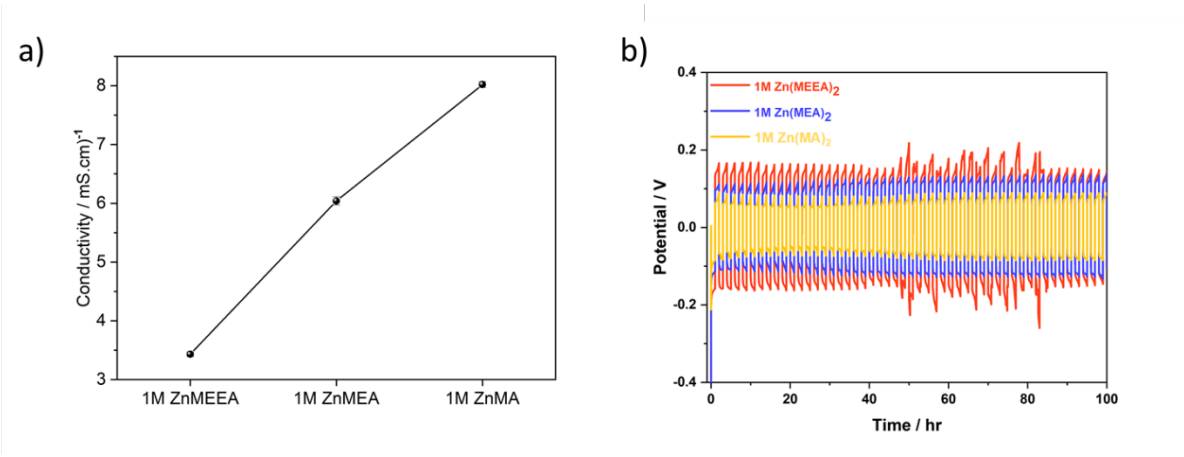

Fig. S8 – a) Ionic conductivity for $Zn(MA)_2$, $Zn(MEA)_2$ and $Zn(MEEA)_2$ and b) Zn || Zn symmetric cells for 1 M $Zn(MA)_2$ (orange), 1 M $Zn(MEA)_2$ (blue) and 1 M $Zn(MEEA)_2$ (red).

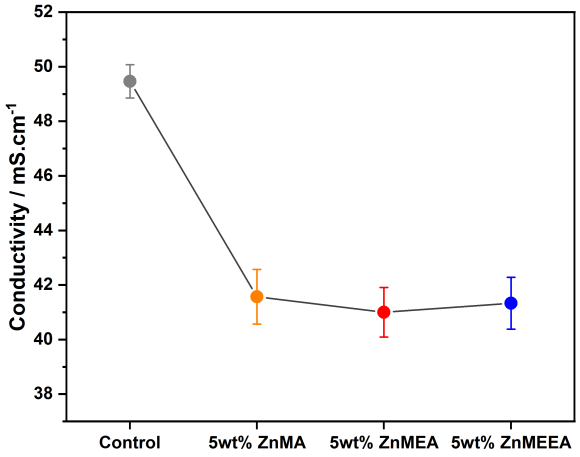

Fig. S9 – Ionic conductivity for 2M $ZnSO_4$, 5wt% $Zn(MA)_2$, $Zn(MEA)_2$ and $Zn(MEEA)_2$ in 2M $ZnSO_4$

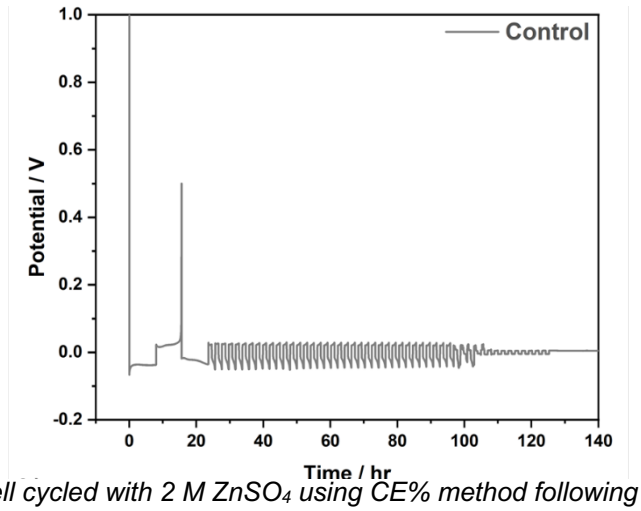

Fig. S10 – Zn || Cu cell cycled with 2 M $ZnSO_4$ using CE% method following Xu et al. which failed

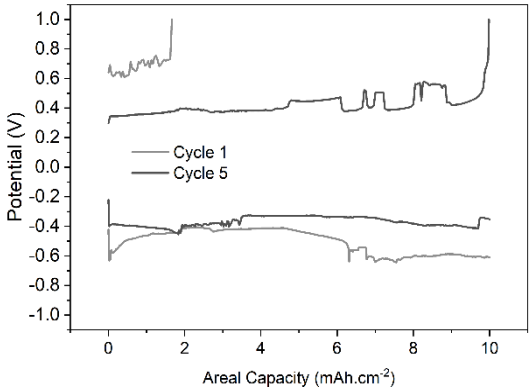

Fig. S11 – Zn || Cu cell cycled with 2 M $ZnSO_4$ at 5 mA.cm^{-2} / 10 mAh.cm^{-2}

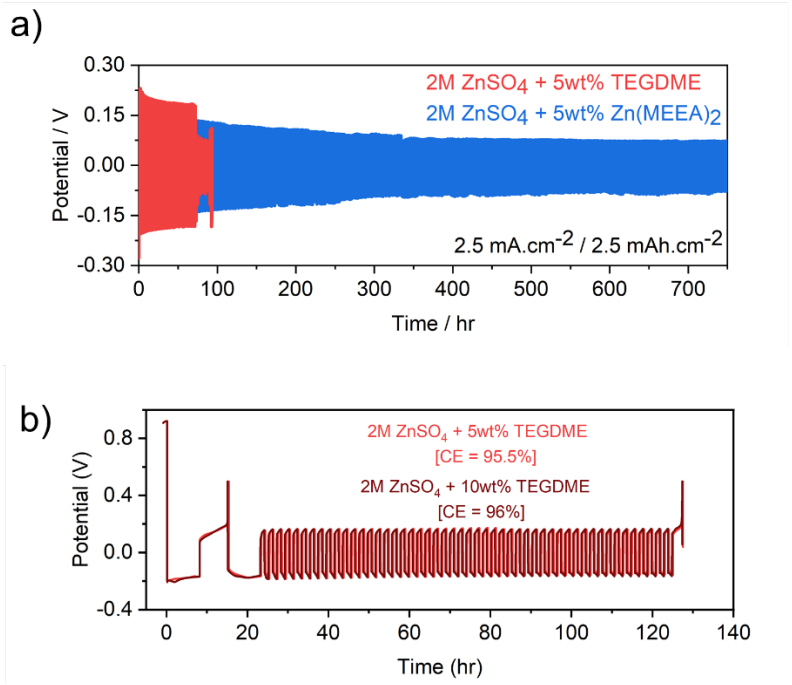

Fig. S12 – a) Zn || Zn cells for 2 M $ZnSO_4$ + 5wt% $Zn(MEEA)_2$ (blue) and 2M ZnSO4 + 5wt% TEGDME at 0.624 mA.cm^{-2} / 2.5 mAh.cm^{-2} & b) CE% determination with 2 M $ZnSO_4$ + 5 and 10 wt% TEGDME in Zn || Cu.

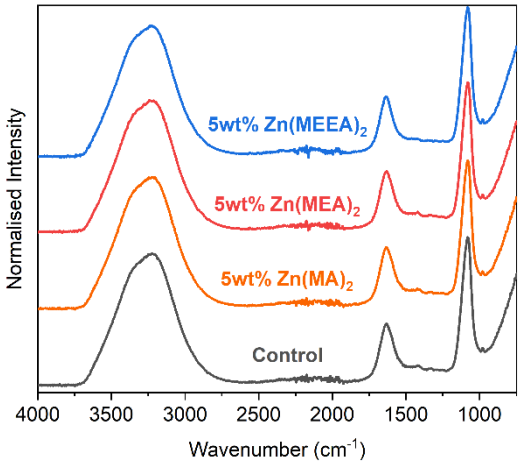

Fig. S13 – a) FT-IR of 2 M $ZnSO_4$ (grey), 2 M $ZnSO_4$ + 5wt% $Zn(MEC)_2$ (orange), 2 M $ZnSO_4$ + 5wt% $Zn(MEA)_2$ (red) and 2 M $ZnSO_4$ + 5wt% $Zn(MEEA)_2$ (blue)

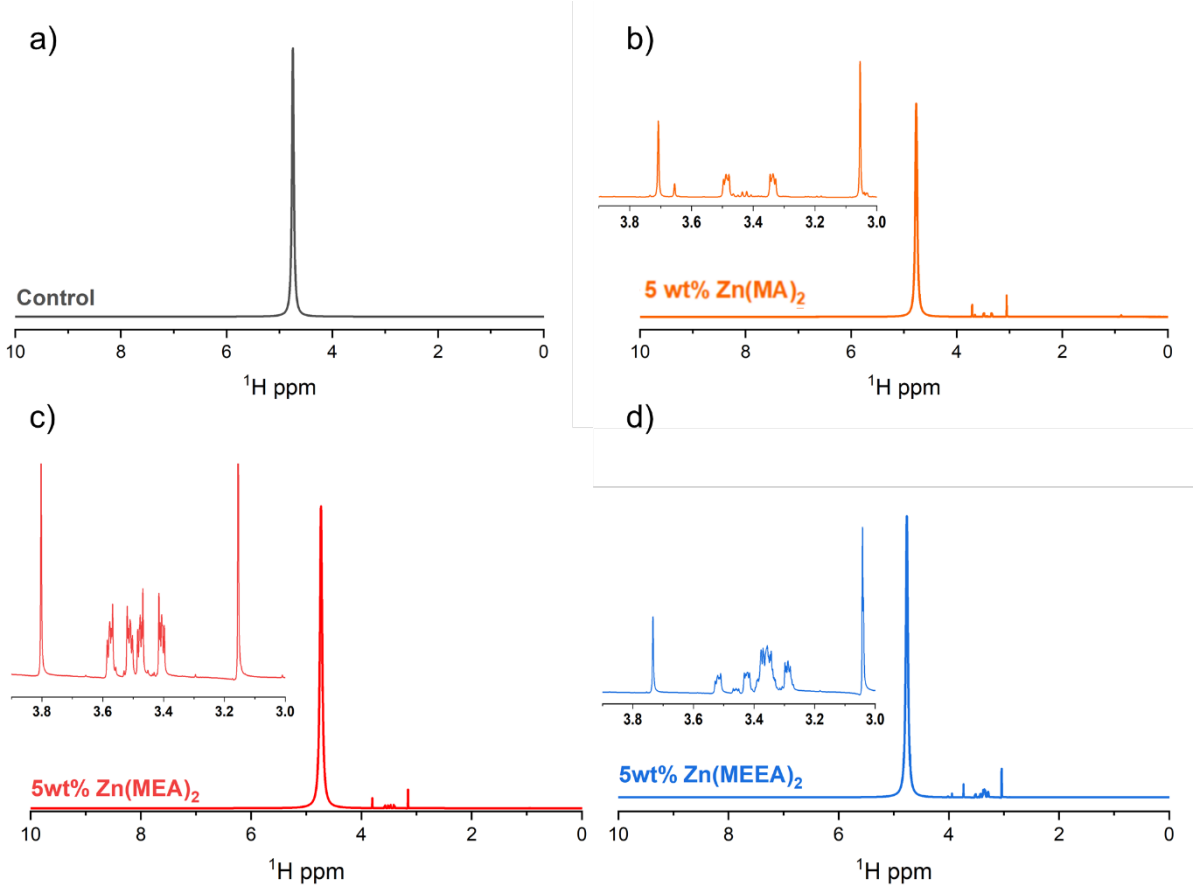

Fig. S14 - a) ^1H NMR for 2 M $ZnSO_4$, b) ^1H NMR 2 M $ZnSO_4$ + 5wt% $Zn(MA)_2$ c) ^1H NMR 2 M $ZnSO_4$ + 5wt% $Zn(MEA)_2$ and d) ^1H NMR 2 M $ZnSO_4$ + 5wt% $Zn(MEEA)_2$.

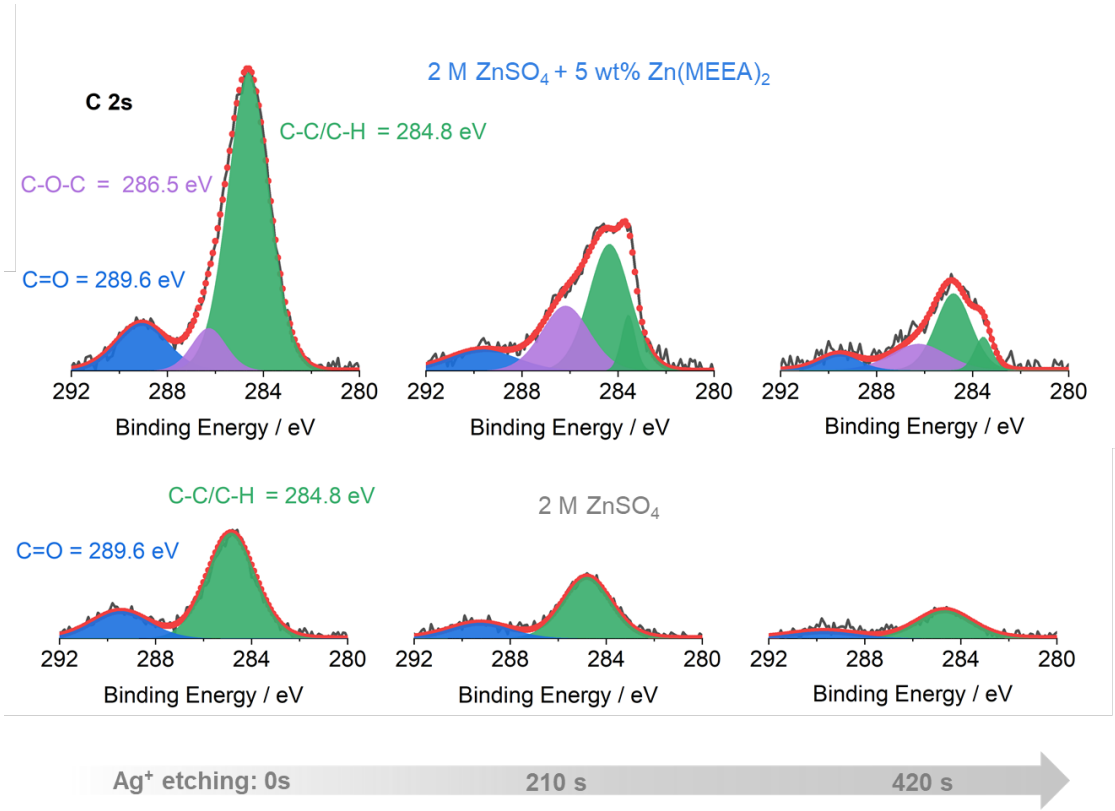

Fig. S15 – C 2s XPS spectra for Zn anodes cycled in 2 M $ZnSO_4$ + 5wt% $Zn(MEEA)_2$ (top) and 2 M $ZnSO_4$ (bottom) with Ag^+ ion beam up to a depth of ~10 nm.

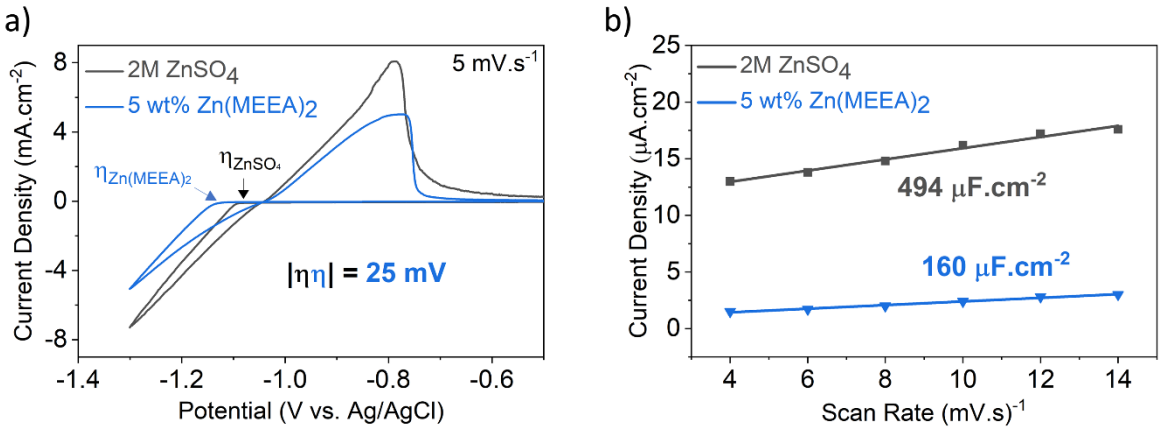

Fig. S16 a) cyclic voltammetry of electrolytes at 5 mV/s on glassy carbon (WE), Pt wire (CE) and Ag/AgCl leakless electrode (REF) for 2 M $ZnSO_4$ & $Zn(MEEA)_2$ & b) EDLC of 2 M $ZnSO_4$ & 5wt% $Zn(MEEA)_2$

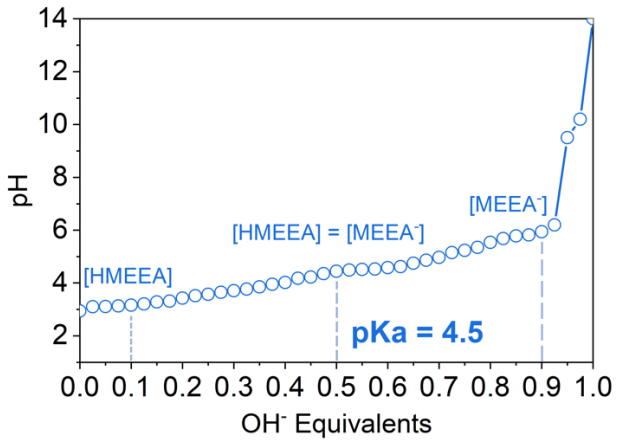

Fig. S17 – Titration of HMEEA

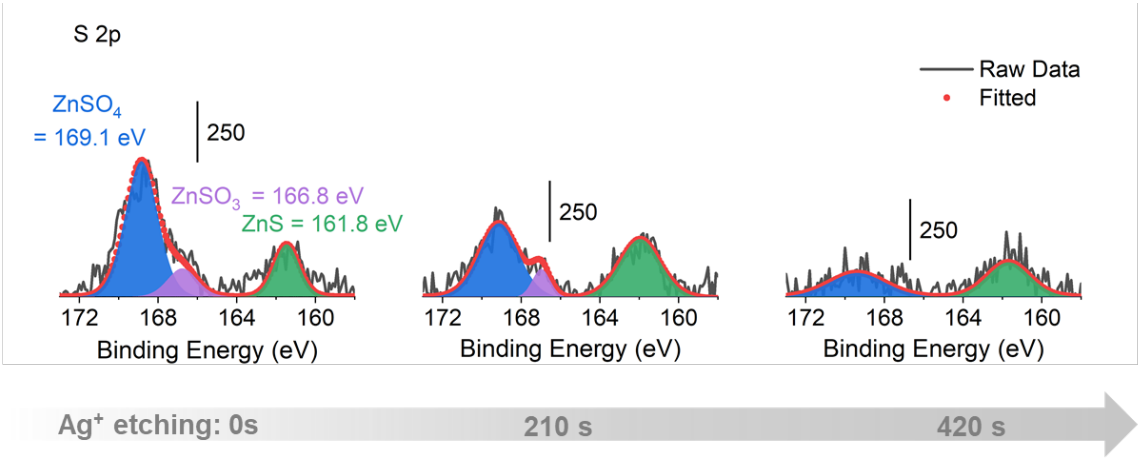

Fig. S18 – S 2p XPS spectra for Zn anodes cycled in 2 M $ZnSO_4$ + 10 M Urea + 5wt% $Zn(MEEA)_2$

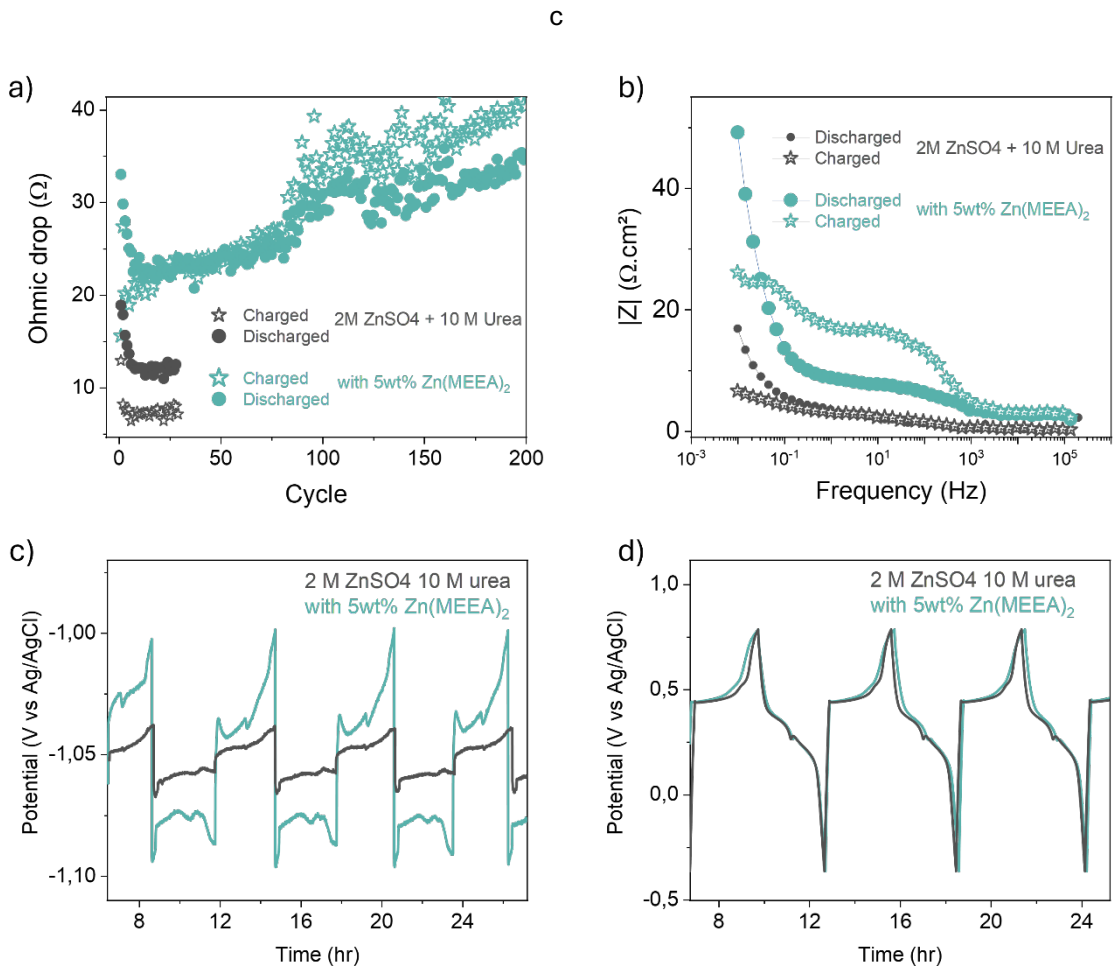

Fig. S19. (a) Ohmic drop of the full cell shown in Fig. 6b after charge and discharge states. (b) Electrochemical impedance of the Zn anode measured in a three-electrode configuration, with and without $Zn(MEEA)_2$. (c) Potential of the zinc foil (reference/counter electrode) during galvanostatic cycling in Zn/MnO_2 three-electrode cells, with and without $Zn(MEEA)_2$. (d) Potential vs. time of the MnO_2 working electrode with and without $Zn(MEEA)_2$ additives.

Ref.	Electrolyte	Current Density ($mA.cm^{-2}$)	Areal Capacity ($mAh.cm^{-2}$)	Cumulative Capacity ($mAh.cm^{-2}$)
2M $ZnSO_4$ + 5wt% $Zn(MEEA)_2$		**5**	**10**	**2500**
1	1m $ZnSO_4$ + 0.1m HTFSI[1]	4	2	1100
2	2M $ZnSO_4$ + 0.05M DOTf[2]	4	4	1000
3	1 M $ZnSO_4$ + 0.5wt% PEO[3]	1	1	1500
4	2M $ZnSO_4$ + 20mM PMS[4]	10	10	2000
5	2M $ZnSO_4$ + 5mM PV[5]	1	1	300

Table 1. Comparison of $Zn(MEEA)_2$ additive to literature.

1. Luo, J. *et al.* Stable zinc anode solid electrolyte interphase via inner Helmholtz plane engineering. *Nat Commun* 15, 6471 (2024).
2. Li, C. *et al.* Highly reversible Zn anode with a practical areal capacity enabled by a sustainable electrolyte and superacid interfacial chemistry. *Joule* 6, 1103–1120 (2022).
3. Jin, Y. *et al.* Stabilizing Zinc Anode Reactions by Polyethylene Oxide Polymer in Mild Aqueous Electrolytes. *Adv Funct Mater* 30, 2003932 (2020).
4. Song, Y. *et al.* Bilateral in-situ functionalization towards Ah-scale aqueous zinc metal batteries. *Nat Commun* 16, 3142 (2025).
5. Liang, W. *et al.* Electrolyte Engineering Strategy with Catecholate Type Additive Enabled Ultradurable Zn Anode. *Adv Funct Mater* n/a, 2504195.